ARTICLE OPEN

Check for updates

Genetic, individual, and familial risk correlates of brain network controllability in major depressive disorder

Tim Hahn [1✉], Nils R. Winter [1], Jan Ernsting [1,2], Marius Gruber[1], Marco J. Mauritz[1], Lukas Fisch[1], Ramona Leenings[1,2], Kelvin Sarink [1], Julian Blanke[1], Vincent Holstein[1], Daniel Emden [1], Marie Beisemann[3], Nils Opel[1,4], Dominik Grotegerd[1], Susanne Meinert[1,5], Walter Heindel[6], Stephanie Witt [7], Marcella Rietschel [7], Markus M. Nöthen [8], Andreas J. Forstner [8], Tilo Kircher[9], Igor Nenadic[9], Andreas Jansen[9,10], Bertram Müller-Myhsok[11], Till F. M. Andlauer [12], Martin Walter [13], Martijn P. van den Heuvel[14,15], Hamidreza Jamalabadi[9], Udo Dannlowski [1,17] and Jonathan Repple [1,16,17]

Many therapeutic interventions in psychiatry can be viewed as attempts to influence the brain's large-scale, dynamic network state transitions. Building on connectome-based graph analysis and control theory, Network Control Theory is emerging as a powerful tool to quantify network controllability—i.e., the influence of one brain region over others regarding dynamic network state transitions. If and how network controllability is related to mental health remains elusive. Here, from Diffusion Tensor Imaging data, we inferred structural connectivity and inferred calculated network controllability parameters to investigate their association with genetic and familial risk in patients diagnosed with major depressive disorder (MDD, $n = 692$) and healthy controls ($n = 820$). First, we establish that controllability measures differ between healthy controls and MDD patients while not varying with current symptom severity or remission status. Second, we show that controllability in MDD patients is associated with polygenic scores for MDD and psychiatric cross-disorder risk. Finally, we provide evidence that controllability varies with familial risk of MDD and bipolar disorder as well as with body mass index. In summary, we show that network controllability is related to genetic, individual, and familial risk in MDD patients. We discuss how these insights into individual variation of network controllability may inform mechanistic models of treatment response prediction and personalized intervention-design in mental health.

INTRODUCTION

Complex network theory conceptualizes the brain as a dynamical system which depends on the interactions between distributed brain regions [1]. Accordingly, the brain can be viewed as an intricate network of brain regions that synchronize their activity via anatomical and functional connections. Based on this, mathematical graph theory is utilized to gain insights into the underlying organizational principles of the brain [2, 3] and its topological organization in health and disease [4, 5]. For example, reduced global fractional anisotropy (FA) has been associated with remission status of depressive patients, while FA in connections between frontal, temporal, insular, and parietal regions was found to be negatively associated with symptom severity [6, 7]. Cross-disorder connectome analyses have further revealed disruptions in connections central to global network communication and

integration, emphasizing the involvement of the connectome in a wide range of mental health and neurological conditions [8]. In addition, machine learning on graphs—for example graph convolutional networks or reinforcement learning-based graph dismantling [9]—is emerging as a fruitful extension of classical graph analysis.

While classic connectome analysis has yielded tremendous insights into the topological organization of the brain in health and disease, it does not advance our ability to actively manipulate and control the brain. It is, however, this very ability to control the large-scale dynamics of the brain which facilitates virtually all therapeutic interventions in psychiatry [10, 11]. In short, any intervention—from medication to psychotherapy—can be conceptualized as an attempt to control the large-scale, dynamic network state transitions in the brain [1, 12, 13]. Control Theory as

the study and practice of controlling dynamical systems is ubiquitous in medicine and biology [14], framing any intervention—from the optimization of cancer chemotherapy [15, 16] and the design of artificial organs [17] to real-time drug administration and non-pharmaceutical pandemic defense strategies [18]—as a control problem.

Integrating Control Theory and network neuroscience, recent progress in Network Control Theory has enabled the quantification of the influence a brain region has on the dynamic transitions between brain states [1, 12]. This so-called controllability of a brain region is linked to its structural connectivity properties which constrain or support transitions between different brain states [19, 20] and has been strongly related to a multitude of cognitive domains [20]. Controllability of a brain region is commonly captured by two key metrics: On the one hand, average controllability measures the ability of a system to spread and amplify the control inputs and is thus indicative of the node's ability to support low-energy state transitions. On the other hand, modal controllability represents the ability to control especially fast decaying neural dynamics [21]. For formal definitions of average and modal controllability measures see Methods section.

Elucidating the variation and effect of controllability in mental disorders is of particular interest as controlling large-scale state transitions in the brain that underly cognition and behavior is at the heart of all therapeutic interventions in psychiatry [1, 22]. Fueled by evidence that the human brain is in principle controllable [19] and the recently discovered associations with cognition [20, 23], studies with small to moderate patient sample sizes have begun to investigate network controllability in mental disorders. First, Jeganathan et al. [24] showed altered controllability in young people with bipolar disorder ($n = 38$) and those at high genetic risk ($n = 84$) compared to healthy controls ($n = 96$). Likewise, Braun et al. [25] showed altered network control properties in schizophrenia patients ($n = 24$) as compared to ($n = 178$) healthy controls. Of note, Parkes et al. [26] investigated the association between average controllability and negative and positive psychosis spectrum symptoms in a large sample of youths between 8 and 22 years of age. Related to mental disorders, Kenett et al. [27] showed regional associations between controllability and subclinical depressive symptoms as measured using the Beck Depression Inventory [28] in healthy controls.

Building on these advances, we provide a comprehensive characterization of individual variation in average and modal controllability regarding demographic, disease-related, genetic, personal, and familial risk in Major Depressive Disorder (MDD). First, we assess the effect of age and gender on average and modal controllability. Then, we compare average and modal controllability between healthy controls and MDD patients and test whether these measures vary with age, gender, current symptom severity, or remission status. Second, we assess whether average and modal controllability in MDD patients are associated with polygenic scores for MDD [29], Bipolar Disorder [30], and psychiatric cross-disorder [31] risk as well as with familial risk of MDD and bipolar disorder. Finally, we quantify the effects of body mass index as a personal risk factors previously reported to be associated with brain-structural deviations in MDD on average and modal controllability [32, 33].

METHODS AND MATERIALS
Sample
Participants were part of the Marburg-Münster Affective Disorders Cohort Study (MACS) [34] and were recruited at two different sites (Marburg & Münster, Germany). See [35] for a detailed description of the study protocol. Participants ranging in age from 18 to 65 years were recruited through newspaper advertisements and local psychiatric hospitals. All experiments were performed in accordance with the ethical guidelines and regulations and all participants gave written

Table 1. Sample summary.

Characteristic	MDD[a] ($n = 692$)	HC[a] ($n = 820$)	p
Sociodemographic			
Gender	451 female, 241 male	529 female, 291 male	<0.001[b]
Age, years	36.41 ± 13.13	33.96 ± 12.75	<0.001[c]
Questionnaires			
BDI	17.67 ± 11.06	4.02 ± 4.18	<0.001[c]
Clinical			
Depressive episodes	3.86 ± 6.28	–	–
Duration of illness, years	10.27 ± 9.75	–	–
Medication			
Medication load	1.32 ± 1.47	–	–
CPZ	24.77 ± 89.21	–	–

HC healthy control group, *MDD* patient group with major depression disorder, *BDI* sum score based on 21 items, *CPZ* chlorpromazine-equivalent doses.
[a]Numbers present either absolute numbers or mean plus standard deviation.
[b]χ2-test (two-tailed).
[c]t-test (two-tailed).

informed consent prior to examination. To confirm the psychiatric diagnosis or a lack thereof, the Structural Clinical Interview for Diagnostic and Statistical Manual of Mental Disorders-IV Text Revision (DSM-IV-TR) (SCID-I [36];) was used. MDD subjects were included with current acute depressive episodes and partial or full remission from depression. Patients could be undergoing in-patient, out-patient, or no current treatment at all. Exclusion criteria comprised the presence of any neurological abnormalities, history of seizures, head trauma or unconsciousness, severe physical impairment (e.g. cancer, unstable diabetes, epilepsy etc.), pregnancy, hypothyroidism without adequate medication, claustrophobia, color blindness, and general MRI contraindications (e.g. metallic objects in the body). Only Caucasian subjects were included in the analyses. Further, lifetime diagnoses of schizophrenia, schizoaffective disorder, bipolar disorder, or substance dependence posed reason for exclusion. After excluding subjects according to the aforementioned exclusion criteria, DTI data for 1567 subjects were available. 55 subjects were excluded due to poor DTI quality (see below for a detailed description of the quality assurance procedure). Final samples of $n = 692$ MDD patients and $n = 820$ healthy controls were used for the controllability analyses. See Table 1 for a sample description of sociodemographic and clinical data.

Imaging data acquisition
In the MACS Study, two MR scanners were used for data acquisition located at the Departments of Psychiatry at the University of Marburg and the University of Münster with different hardware and software configurations. Both T1 and DTI data were acquired using a 3 T whole body MRI scanner (Marburg: Tim Trio, 12-channel head matrix Rx-coil, Siemens, Erlangen, Germany; Münster: Prisma, 20-channel head matrix Rx-coil, Siemens, Erlangen, Germany). A GRAPPA acceleration factor of two was employed. For DTI imaging, fifty-six axial slices, 2.5 mm thick with no gap, were measured with an isotropic voxel size of $2.5 \times 2.5 \times 2.5$ mm^3 (TE = 90 ms, TR = 7300 ms). Five non-DW images (b0 = 0) and 2×30 DW images with a *b*-value of 1000 sec/mm² were acquired. Imaging pulse sequence parameters were standardized across both sites to the extent permitted by each platform. For a description of MRI quality control procedures see [35]. The body coil at the Marburg scanner was replaced during the study. Therefore, a variable modeling three scanner sites (Marburg old body coil, Marburg new body coil and Münster) was used as covariate for all statistical analyses.

Imaging data preprocessing

Connectomes were reconstructed involving the following steps [37]. For a more detailed description of the preprocessing see [6]. In accordance with [6], we decided on using a basic DTI reconstruction rather than more advanced diffusion direction reconstruction methods to provide a reasonable balance between false negative and false positive fiber reconstructions [38]. For each subject an anatomical brain network was reconstructed, consisting of 114 areas of a subdivision of the FreeSurfer's Desikan–Killiany atlas [39, 40], and the reconstructed streamlines between these areas. White matter connections were reconstructed using deterministic streamline tractography, based on the Fiber Assignment by Continuous Tracking (FACT) algorithm [41]. Network connections were included when two nodes (i.e., brain regions) were connected by at least three tractography streamlines [42]. For each participant, the network information was stored in a structural connectivity matrix, with rows and columns reflecting cortical brain regions, and matrix entries representing graph edges. Edges were only described by their presence or absence to create unweighted graphs.

DTI quality control

In accordance with [6], measures for outlier detection included 1. average number of streamlines, 2. average fractional anisotropy, 3. average prevalence of each subject's connections (low value, if the subject has "odd" connections), and 4. average prevalence of each subjects connected brain regions (high value, if the subject misses commonly found connections). For each metric the quartiles (Q1, Q2, Q3) and the interquartile range (IQR = Q3–Q1) was computed across the group and a datapoint was declared as an outlier if its value was below $Q1 - 1.5 \times IQR$ or above $Q3 + 1.5 \times IQR$ on any of the four metrics.

Genotyping and calculation of polygenic scores

Genotyping was conducted using the PsychArray BeadChip (Illumina, San Diego, CA, USA), followed by quality control and imputation, as described previously [43, 44]. In brief, quality control and population substructure analyses were performed in PLINK v1.90 [45], as described in the Supplementary Methods. The data were imputed to the 1000 Genomes phase 3 reference panel using SHAPEIT and IMPUTE2.

For the calculation of polygenic risk scores (PRS; [46]), single-nucleotide polymorphism (SNP) weights were estimated using the PRS-CS method [47] with default parameters. This method employs Bayesian regression to infer PRS weights while modeling the local linkage disequilibrium patterns of all SNPs using the EUR super-population of the 1000 Genomes reference panel. The global shrinkage parameter φ was determined automatically (PRS-CS-auto; CD: $\varphi = 1.80 \times 10^{-4}$, MDD: $\varphi = 1.11 \times 10^{-4}$). The PRS were calculated, using these weights, in PLINK v1.90 on imputed dosage data based on summary statistics of genome-wide association studies (GWAS) by the Psychiatric Genomics Consortium (PGC) containing 162,151 cases and 276,846 controls for a cross-disorder phenotype [31] and 59,851 cases and 113,154 controls for MDD [29]. PRS were available for 637 of the 692 MDD patients.

Network controllability analysis

To assess the ability of a certain brain region to influence other regions in different ways, we adopt the control theoretic notion of controllability. Controllability of a dynamical system refers to the possibility of driving the state of a dynamical system to a specific target state by means of an external control input [48]. A state is defined as the vector of neurophysiological activity magnitudes across brain regions at a single time point. In this paper, following the established model of structural brain controllability [19], we assume the system to follow a descrete noise-free linear time-invariant model as in Eq. 1.

$$x(k + 1) = Ax(k) + Bu(k) \tag{1}$$

where x represents the temporal activity of the 114 brain regions, A is the adjacency matrix whose elements quantify the structural connectivity between every two brain regions, B is the input matrix and u shows the control strategy. Classic results in control theory ensure that the system in Eq. 1 is from the set of nodes K controllable, when the controllability Gramian matrix $W_K = \sum_{i=0}^{\infty} A^i B_K B_K^T (A^T)^i$ is invertible (T denotes matrix transpose). A rigorous mathematical formulation of network controllability in brain networks can be found in [19]. From the Gramian matrix, different controllability measures can be computed for each node (brain region) in the network. Here, based on previous research of network controllability in brain networks, we compute for each participant and each brain region their average controllability and modal controllability as defined in [19].

Average controllability, estimated as the trace of the controllability Gramian matrix i.e. $Tr(W_j)$ where $B = e_j$ is the jth canonical vector (all elements except for the jth item are zero)., is a measure of the ability of brain regions to spread the control inputs. Thus, regions with high average controllability can be used to drive the brain towards a greater number of reachable and nearby states. Previous work has identified brain regions that demonstrate high average controllability, such as the precuneus, posterior cingulate, superior frontal, paracentral, precentral, and subcortical structures [19].

Modal controllability (MC) is a measure of the ability of brain regions to control the fast decaying modes of brain activity and thus those states that are intuitively more difficult to reach. Mathematically, MC is estimated as $\phi_j = \sum_n^N \left[1 - \xi_n^2(A) \right] v_{nj}^2$ where ξ_j and v_{nj} represent respectively the eigenvalues and elements of the eigenvector matrix of A ($N = 114$). Previous work has identified brain regions that demonstrate high modal controllability, such as the postcentral, supramarginal, inferior parietal, pars orbitalis, medial orbitofrontal, and rostral middle frontal cortices [19].

Building on these definitions, we estimate single node controllability measures (average and modal controllability) and the whole-brain controllability is then defined as the average of single node controllability metrics over all nodes.

Statistical analyses

Our analysis process is as follows (Fig. 1): Based on DTI data (Fig. 1a), we defined anatomical brain networks by subdividing the entire brain into 114 anatomically distinct brain regions (network nodes) in a commonly used
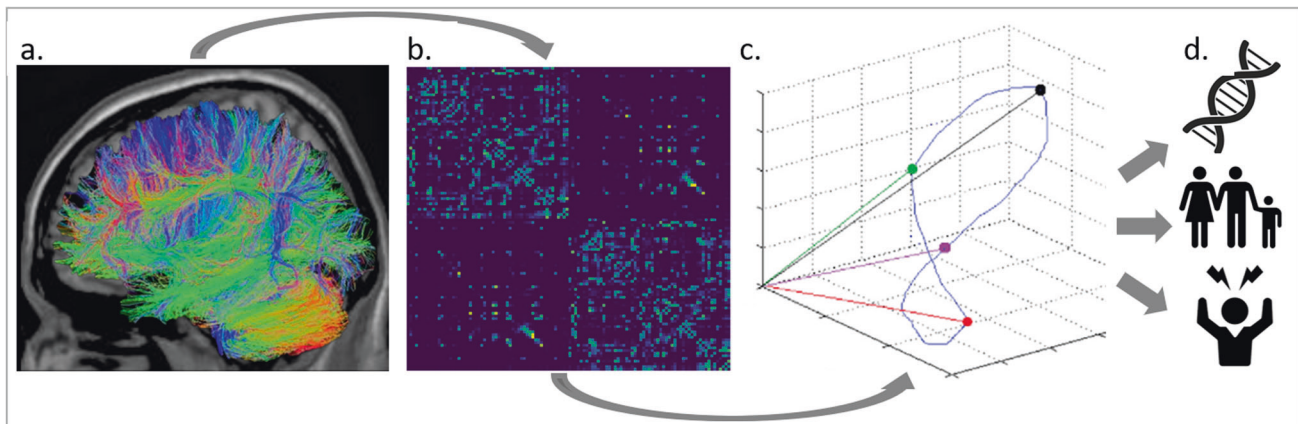

Fig. 1 Analysis Overview. From Diffusion Tensor Imaging data (**a**) we derived the structural connectivity matrix for each participant (**b**) and quantified modal and average controllability—i.e., the influence a brain region has on the dynamic transitions between brain states underlying cognition and behavior (**c**). We then investigated their association with genetic, familial, and personal risk (**d**).

anatomical atlas [39, 40]. Following prior work (see "Imaging data preprocessing"), we connected nodes (brain regions) by the number of white matter streamlines which results in sparse, undirected structural brain networks for each participant (Fig. 1b). Next, a simplified model of brain dynamics was applied to simulate network control and quantify average and modal controllability for each brain region for each participant, as described in [19, 48]. Figure 1c illustrates the dynamic state transitions of the brain over time. Note that in our analyses, a brain state is characterized not by three, but 114 values per time point, corresponding to the 114 regions contained in the atlas. Points in this space (colored points in Fig. 1c) thus correspond to brain states at different time points. Controllability parameters are, in turn, related to the ease with which a given brain region can induce dynamic state transitions in this space (see "Network controllability analysis").

We then analyzed mean whole-brain controllability as well as regional (i.e., per-node) controllability (dependent variable) using an ANCOVA approach with age, gender, MRI scanner site, and the number of present edges as covariates. For all analyses involving PRS, we also controlled for ancestry (first three MDS components). Also, we removed outliers defined as values located more than three standard deviations from the mean. In all analyses involving MDD patients only, we additionally controlled for medication load in accordance with previous publications [6, 49]. We report partial η^2 as effect size for all whole-brain analyses and provide the 95% confidence interval based on 1000 draws with replacement. Note that, in the regional analyses, we controlled for multiple comparisons by calculating the false discovery rate [50] with a false-positive rate of 0.05. All other constructs (age, gender, diagnosis, symptom severity, familial risk of MDD and BD as well as polygenic scores for MDD, BD, and cross-disorder risk) were tested independently and not corrected further for multiple testing.

RESULTS
Demographic effects
First, we examined whether chronological age and gender are associated with controllability as has been shown before [23, 51]. Indeed, we find that the *whole-brain average controllability* was negatively correlated with age for both healthy controls ($F(1,811) = 24.47$, $p < 0.001$, $\eta p^2 = 0.029292$ [0.012970, 0.051426]) and MDD patients ($F(1,686) = 15.08$, $p < 0.001$, $\eta p^2 = 0.021505$ [0.007166, 0.043462]). Likewise, the regional average controllability significantly varied with age in 30 and 35 different regions for healthy controls and MDD patients, respectively (all $p < 0.05$, FDR-corrected; for a full list of regions for all analyses yielding significant regional associations, see Supplementary Results Tables S1 to S16). *Whole-brain modal controllability* was positively correlated with age for both healthy controls ($F(1,811) = 3.93$, $p = 0.048$, $\eta p^2 = 0.004821$ [0.000101, 0.016141]) and showed a similar trend in MDD patients ($F(1,685) = 2.91$, $p = 0.089$, $\eta p^2 = 0.004229$ [0.000124, 0.015783]). Regional modal controllability significantly varied with age in 33 regions for both healthy controls and MDD patients (all $p < 0.05$, FDR-corrected). Gender was not significantly associated with *whole-brain average controllability* for healthy controls ($F(1,814) = 0.04$, $p = 0.839$, $\eta p^2 = 0.000051$ [0.000004, 0.004761]) or MDD patients ($F(1,687) = 0.08$, $p = 0.773$, $\eta p^2 = 0.000121$ [0.000003, 0.006214]). In contrast, regional average controllability significantly varied with gender in 12 and 13 regions for healthy controls and MDD patients, respectively (all $p < 0.05$, FDR corrected). Whole-brain modal controllability was higher in males than in females for healthy controls ($F(1,814) = 7.58$, $p = 0.006$, $\eta p^2 = 0.009231$ [0.001672, 0.022200]) and showed a similar trend in MDD patients ($F(1,687) = 3.73$, $p = 0.054$, $\eta p^2 = 0.005397$ [0.000222, 0.019111]). Regional modal controllability significantly varied with age in 16 and 18 regions for healthy controls and MDD patients, respectively (all $p < 0.05$, FDR corrected).

Disease-related variation
Focusing specifically on controllability in MDD, we show that patients displayed lower whole-brain *modal controllability*

($F(1,1505) = 7.96$, $p = 0.005$, $\eta p^2 = 0.005261$ [0.001227, 0.012531]) than healthy controls. Correspondingly, we observed a non-significant trend towards higher whole-brain *average controllability* values in MDD patients ($F(1,1505) = 3.08$, $p = 0.080$, $\eta p^2 = 0.002041$ [0.000056, 0.007247]).

In contrast to previous findings in sub-clinically depressed controls [27], our results do not support an effect of current symptom severity, as measured by the Beck Depression Inventory, on the whole-brain *average* ($F(1,671) = 0.19$, $p = 0.665$, $\eta p^2 = 0.000279$ [0.000005, 0.006632]) or *modal* controllability ($F(1,671) = 1.49$, $p = 0.222$, $\eta p^2 = 0.002222$ [0.000038, 0.011509]) in MDD patients. In line with this observation, the remission status was neither associated with *average* ($F(2,683) = 0.43$, $p = 0.649$, $\eta p^2 = 0.001264$ [0.000188, 0.013090]) nor *modal controllability* ($F(2,683) = 0.07$, $p = 0.935$, $\eta p^2 = 0.000196$ [0.000229, 0.009890]) on the whole-brain or regional level in MDD patients. For direct comparison with the previous publication, we also analyzed the healthy controls only: Again, we did not find a significant association between current symptom severity and whole-brain *average* ($F(1,793) = 0.86$, $p = 0.355$, $\eta p^2 = 0.001080$ [0.000014, 0.008154]) or *modal* controllability ($F(1,793) = 2.32$, $p = 0.128$, $\eta p^2 = 0.002923$ [0.000053, 0.012674]).

Genetic and familial risk factors
Next, we examined whether controllability in MDD patients is associated with familial risk of MDD and Bipolar Disorder. We show that *average controllability* was significantly higher in patients carrying self-reported familial risk of MDD ($F(1,685) = 4.87$, $p = 0.028$, $\eta p^2 = 0.007064$ [0.000485, 0.022823]), mirroring the trend-wise increased average controllability of MDD patients compared to healthy controls. This was not the case for *modal controllability* ($F(1,685) = 2.40$, $p = 0.122$, $\eta p^2 = 0.003492$ [0.000070, 0.015817]).

Average controllability was also higher in patients carrying a familial risk of Bipolar Disorder ($F(1,685) = 10.30$, $p = 0.001$, $\eta p^2 = 0.014809$ [0.002123, 0.038855]) with regional effects in the right supramarginal gyrus, right inferior parietal gyrus, and precuneus. Likewise, whole-brain *modal controllability* was lower in patients carrying a familial risk of Bipolar Disorder ($F(1,685) = 9.69$, $p = 0.002$, $\eta p^2 = 0.013951$ [0.002281, 0.033644]) with regional effects in the right supramarginal gyrus (for detailed regional analyses, see the Supplementary Tables S15 and S16).

Building on this evidence, we extended the analysis to polygenic risk scores and show that polygenic risk scores for MDD [26] were negatively associated with modal controllability ($F(1,624) = 4.88$, $p = 0.028$, $\eta p^2 = 0.007757$ [0.000446, 0.024640]). Likewise, polygenic risk scores for cross-disorder risk [28] were also negatively associated with whole-brain modal controllability ($F(1,623) = 4.17$, $p = 0.042$, $\eta p^2 = 0.006650$ [0.000322, 0.021361]). In addition, we show that polygenic risk scores for MDD [26] were positively correlated with average controllability ($F(1,623) = 3.86$, $p = 0.050$, $\eta p^2 = 0.006164$ [0.000287, 0.021261]). Polygenic risk scores for cross-disorder risk [28] were not significantly associated with whole-brain average controllability ($F(1,622) = 0.99$, $p = 0.320$, $\eta p^2 = 0.001590$ [0.000012, 0.011372]).

In contrast to the observed effect for familial risk of Bipolar Disorder, we neither found a significant association of average ($F(1,624) = 0.21$, $p = 0.644$, $\eta p^2 = 0.000342$ [0.000006, 0.007621]) nor modal controllability ($F(1,623) = 0.00$, $p = 0.990$, $\eta p^2 = 0.000000$ [0.000011, 0.007404]) with polygenic risk score for Bipolar Disorder [30].

Body mass index
With mounting evidence pointing towards brain-structural deviations relating body mass index and MDD [32, 33], we examined the effects of body mass index on controllability. For average controllability, we found associations in 9 regions ($p < .05$, FDR corrected) including negative correlations in the left superior

frontal and posterior cingulate gyrus as well as positive correlations in the superior temporal and left lingual gyrus (see Supplementary Tables S13 und S14). With positive and negative regional associations, a whole-brain effect was absent ($F_{(1,643)} = 0.31$, $p = 0.579$, $\eta p^2 = 0.000478$ [0.000008, 0.007147]). Analyses of modal controllability revealed the involvement of 6 regions ($p < 0.05$, FDR-corrected) showing a similar set of regions including the left superior frontal, posterior cingulate, and superior temporal gyrus with—as expected—a switched direction of correlations and, again, no consistent whole-brain effect ($F_{(1,684)} = 1.10$, $p = 0.294$, $\eta p^2 = 0.001611$ [0.000014, 0.011596]).

To assess the specificity of our results, we additionally tested for the association with height and participant order of inclusion in the study. Neither height (modal controllability: $F_{(1,1410)} = 0.88$, $p = 0.349$, $\eta p^2 = 0.000622$ [0.000008, 0.004492]) nor order of inclusion ($F_{(1,1410)} = 0.41$, $p = 0.522$, $\eta p^2 = 0.000290$ [0.000004, 0.003831]) showed any significant effects on the whole-brain or on the regional level.

DISCUSSION
Building on Network Control Theory, we investigated the association of average and modal network controllability with genetic, familial, and individual risk in MDD patients ($n = 692$) and healthy controls ($n = 820$). First, we established that controllability measures differ between healthy controls and MDD patients while not varying with current symptom severity or remission status. Second, we showed that modal and average controllability in MDD patients could be predicted based on polygenic scores for MDD and psychiatric cross-disorder risk as well as associations with familial risk of MDD and bipolar disorder. Finally, we provide evidence that controllability varies with body mass index. This evidence suggests that individual differences in these variables either impact the brain's control architecture (e.g., in the case of genetic effects) or are driven by it—as may be the case for e.g. body mass index.

Against this background, our results indicate that individual differences in demographic, disease-related, genetic, individual, and familial risk factors are associated with controllability. We replicated previous findings showing that age and gender affected controllability measures [23, 51] also for MDD patients. Given that women are disproportionally affected by MDD, future studies might investigate gender differences in more detail.

Interestingly, associations were mainly found with whole-brain controllability—modal and average alike—suggesting subtle changes in how effectively not only single regions, but a larger set of regions in the brain can drive state transitions. This is of particular interest as previous studies have focused on the set of 30 regions with the highest controllability defined a priori, thereby potentially obscuring such whole-brain effects. This suggests that extending current controllability analyses towards the investigation of sets of regions controlling the brain (as has been done by, e.g., [52]) might be fruitful also for MDD. Moreover, all results were corrected for the number of present edges, which suggests a specific control effect that goes beyond basic graph properties.

More fundamentally, the question regarding the biological underpinnings of the control theoretic concepts has to be addressed: To this end, He et al. showed that control theoretic constructs are directly linked to gray matter integrity, metabolism, and energetic generation in the brain [53]. Specifically, they showed in temporal lobe epilepsy patients that higher control energy is required to activate the limbic network compared to healthy volunteers. The energetic imbalance between ipsilateral and contralateral temporolimbic regions was tracked by asymmetric patterns of glucose metabolism measured using positron emission tomography, which, in turn, was selectively explained by asymmetric gray matter loss. This work provides the first theoretical framework unifying gray matter integrity, metabolism, and energetic generation in a control theoretic framework. In addition, controllability has been associated with cognition [20, 23] and numerous studies have empirically investigated the two metrics in mental disorders other than MDD [24–26].

From the more general perspective of control, answering what changes in the brain after a specified stimulation event and which regions are most effective or efficient to stimulate is crucial for all therapeutic interventions. First attempts to achieve these goals in the context of electrical brain stimulation have recently shown promising results [54, 55]. In this context, our results imply that individual characteristics may be relevant when designing future interventions based on Network Control Theory. In turn, our results suggest that variation in response to treatment—e.g., with transcranial magnetic stimulation or electroconvulsive therapy—might be explained by controllability differences arising from demographic, disease-related, genetic, personal, and familial risk. Future studies may therefore investigate whether interventions guided by Network Control Theory are more effective or efficient than current approaches.

Several limitations should be noted. First, calculation of average and modal controllability relies on the simplified noise-free linear discrete-time and time-invariant network model employed in virtually all work on brain Network Control Theory [19, 22, 56]. Given the brain's clearly non-linear dynamics, this is justified as 1) nonlinear behavior may be accurately approximated by linear behavior [57] and 2) the controllability of linear and nonlinear systems is related such that a controllable linearized system is locally controllable in the nonlinear case (see also [19] for details).

Second, our estimation of controllability is based upon Diffusion Tensor Imaging (DTI) tractography which in itself is limited in its ability to accurately quantify the structural connectome (for an introduction, see [58]). Currently, several novel approaches to controllability quantification are being explored including estimation from gray matter [59] and resting-state functional dynamics [56]. Empirically comparing and theoretically reconciling results from these methods will be crucial for robust parameter estimation in Network Control Theory studies of the brain. In addition, longitudinal data from DTI, gray matter, and resting-state functional dynamics available from, e.g., the Marburg-Münster Affective Disorders Cohort Study (MACS [35];) will enable us to assess the (differential) reliability of these approaches. In combination with functional Magnetic Resonance Imaging, this approach also provides an opportunity to further characterize the relationship between network control and individual task-related activation [60].

Third, it should be noted that most effect sizes observed in this study were small. Methodologically, however, it has been shown that small samples systematically inflate the apparent effect size, whereas large samples such as this one provide a much more accurate estimate of the true effect size [61]. Most importantly, our characterization of individual differences in controllability in MDD does not consider isolated effects but is supported by a broad range of analyses.

In summary, we build on a growing body of literature studying cognition and psychopathology within the framework of Network Control Theory to show effects of demographic, disease-related, genetic, personal, and familial risk on modal and average controllability in MDD patients. Thereby, we hope to aid future studies employing Network Control Theory to predict treatment response, guide therapeutic planning, and design novel interventions for MDD.

DATA AVAILABILITY

REFERENCES

1. Braun U, Schaefer A, Betzel RF, Tost H, Meyer-Lindenberg A, Bassett DS. From Maps to Multi-dimensional Network Mechanisms of Mental Disorders. Neuron 2018;97:14–31.
2. Breakspear M. Dynamic models of large-scale brain activity. Nat Neurosci. 2017;20:3 2017;20:340–52.
3. Bassett DS, Zurn P, Gold JI. On the nature and use of models in network neuroscience. Nat Rev Neurosci. 2018;19:566–78.
4. Bullmore E, Sporns O. Complex brain networks: graph theoretical analysis of structural and functional systems. Nat Rev Neurosci. 2009;10:186–98.
5. van den Heuvel MP, Sporns O. A cross-disorder connectome landscape of brain dysconnectivity. Nat Rev Neurosci. 2019;20:435–46.
6. Repple J, Mauritz M, Meinert S, de Lange SC, Grotegerd D, Opel N, et al. Severity of current depression and remission status are associated with structural connectome alterations in major depressive disorder. Mol Psychiatry. 2020;25:1550–8.
7. Korgaonkar MS, Fornito A, Williams LM, Grieve SM. Abnormal structural networks characterize major depressive disorder: a connectome analysis. Biol Psychiatry. 2014;76:567–74.
8. de Lange SC, Scholtens LH, van den Berg LH, Boks MP, Bozzali M, Cahn W, et al. Shared vulnerability for connectome alterations across psychiatric and neurological brain disorders. Nat Hum Behav. 2019;3:988–98.
9. Fan C, Zeng L, Sun Y, Liu YY. Finding key players in complex networks through deep reinforcement learning. Nat Mach Intell. 2020;2:317–24.
10. Fornito A, Harrison BJ. Brain connectivity and mental illness. Front Psychiatry. 2012;0:72.
11. Buckholtz JW, Meyer-Lindenberg A. Psychopathology and the human connectome: toward a transdiagnostic model of risk for mental illness. Neuron 2012;74:990–1004.
12. Kim JZ, Bassett DS. Linear Dynamics and Control of Brain Networks. In: He B. editor. Neural Engineering. Cham: Springer; 2020.
13. Uhlhaas PJ, Singer W. Neuronal dynamics and neuropsychiatric disorders: toward a translational paradigm for dysfunctional large-scale networks. Neuron. 2012;75:963–80.
14. Thomas PJ, Olufsen M, Sepulchre R, Iglesias PA, Ijspeert A, Srinivasan M. Control theory in biology and medicine: Introduction to the special issue. Biol Cyber. 2019;113:1–6.
15. Moore H. How to mathematically optimize drug regimens using optimal control. J Pharmacokinet Pharmacodyn. 2018;45:127–37.
16. Swan GW. Role of optimal control theory in cancer chemotherapy. Math Biosci. 1990;101:237–84.
17. Smieja J. Automatic control and feedback loops in biology and medicine. Advances in Intelligent Systems and Computing, vol. 920, Springer Verlag; 2020. p. 3–12.
18. Lin F, Muthuraman K, Lawley M. An optimal control theory approach to non-pharmaceutical interventions. BMC Infect Dis. 2010;10:32.
19. Gu S, Pasqualetti F, Cieslak M, Telesford QK, Yu AB, Kahn AE, et al. Controllability of structural brain networks. Nat Commun. 2015;6:1–10.
20. Lee WH, Rodrigue A, Glahn DC, Bassett DS, Frangou S. Heritability and cognitive relevance of structural brain controllability. Cereb Cortex. 2020;30:3044–54.
21. Karrer TM, Kim JZ, Stiso J, Kahn AE, Pasqualetti F, Habel U, et al. A practical guide to methodological considerations in the controllability. J Neural Eng. 2020.
22. Lynn CW, Bassett DS. The physics of brain network structure, function and control. Nature Reviews. Physics 2019;1:318–32.
23. Cornblath EJ, Tang E, Baum GL, Moore TM, Adebimpe A, Roalf DR, et al. Sex differences in network controllability as a predictor of executive function in youth. Neuroimage 2019;188:122–34.
24. Jeganathan J, Perry A, Bassett DS, Roberts G, Mitchell PB, Breakspear M. Fronto-limbic dysconnectivity leads to impaired brain network controllability in young people with bipolar disorder and those at high genetic risk. Neuroimage Clin. 2018;19:71–81.
25. Braun U, Harneit A, Pergola G, Menara T, Schaefer A, Betzel RF, et al. Brain state stability during working memory is explained by network control theory, modulated by dopamine D1/D2 receptor function, and diminished in schizophrenia. arXiv preprint arXiv:1906.09290. 2019.
26. Parkes L, Moore TM, Calkins ME, Cieslak M, Roalf DR, Wolf DH, et al. Network controllability in transmodal cortex predicts psychosis spectrum symptoms. Biol Psychiatry. 2021;89:S370–S371.
27. Kenett YN, Beaty RE, Medaglia JD. A computational network control theory analysis of depression symptoms. Personal Neurosci. 2018;1:E16.
28. Beck AT, Steer RA, Brown G. Beck Depression Inventory–II (BDI-II) [Database record]. APA PsycTests. https://doi.org/10.1037/t00742-000. 1996.
29. Howard DM, Adams MJ, Clarke TK, Hafferty JD, Gibson J, Shirali M, et al. Genome-wide meta-analysis of depression identifies 102 independent variants and highlights the importance of the prefrontal brain regions. Nat Neurosci. 2019;22:343–52.
30. Stahl EA, Breen G, Forstner AJ, McQuillin A, Ripke S, Trubetskoy V, et al. Genome-wide association study identifies 30 loci associated with bipolar disorder. Nat Genet. 2019;51:793–803.
31. Lee PH, Anttila V, Won H, Feng YCA, Rosenthal J, Zhu Z, et al. Genomic relationships, novel loci, and pleiotropic mechanisms across eight psychiatric disorders. Cell 2019;179:1469–82.e11.
32. Opel N, Thalamuthu A, Milaneschi Y, Grotegerd D, Flint C, Leenings R, et al. Brain structural abnormalities in obesity: relation to age, genetic risk, and common psychiatric disorders: Evidence through univariate and multivariate mega-analysis including 6420 participants from the ENIGMA MDD working group. Mol Psychiatry. 2020;34:36.
33. Opel N, Redlich R, Grotegerd D, Dohm K, Heindel W, Kugel H, et al. Obesity and major depression: Body-mass index (BMI) is associated with a severe course of disease and specific neurostructural alterations. Psychoneuroendocrinology 2015;51:219–26.
34. Kircher T, Wöhr M, Nenadic I, Schwarting R, Schratt G, Alferink J, et al. Neurobiology of the major psychoses: a translational perspective on brain structure and function—the FOR2107 consortium. Eur Arch Psychiatry Clin Neurosci. 2019;269:949–62.
35. Vogelbacher C, Möbius TWD, Sommer J, Schuster V, Dannlowski U, Kircher T, et al. The Marburg-Münster Affective Disorders Cohort Study (MACS): a quality assurance protocol for MR neuroimaging data. Neuroimage 2018;172:450–60.
36. Wittchen H-U, Zaudig M, Fydrich T. SKID. Strukturiertes Klinisches Interview für DSM-IV. Achse I und II. Handanweisung. Göttingen: Hogrefe; 1997.
37. Collin G, van den Heuvel MP, Abramovic L, Vreeker A, de Reus MA, van Haren NEM, et al. Brain /network analysis reveals affected connectome structure in bipolar I disorder. Hum Brain Mapp. 2016. 2016.2. 0 https://doi.org/10.1002/hbm.23017.
38. Sarwar T, Ramamohanarao K, Zalesky A. Mapping connectomes with diffusion MRI: deterministic or probabilistic tractography? Magn Reson Med. 2019;81:1368–84.
39. Hagmann P, Cammoun L, Gigandet X, Meuli R, Honey CJ, Van Wedeen J, et al. Mapping the structural core of human cerebral cortex. PLoS Biol. 2008. https://doi.org/10.1371/journal.pbio.0060159.
40. Cammoun L, Gigandet X, Meskaldji D, Thiran JP, Sporns O, Do KQ, et al. Mapping the human connectome at multiple scales with diffusion spectrum MRI. J Neurosci Methods. 2012. https://doi.org/10.1016/j.jneumeth.2011.09.031.
41. Mori S, Van Zijl PCM Fiber tracking: Principles and strategies - A technical review. NMR Biomed. 2002.
42. de Reus MA, van den Heuvel MP. Estimating false positives and negatives in brain networks. Neuroimage. 2013;70:402–9.
43. Meller T, Schmitt S, Stein F, Brosch K, Mosebach J, Yüksel D, et al. Associations of schizophrenia risk genes ZNF804A and CACNA1C with schizotypy and modulation of attention in healthy subjects. Schizophr Res. 2019;208:67–75.
44. Andlauer TFM, Buck D, Antony G, Bayas A, Bechmann L, Berthele A, et al. Novel multiple sclerosis susceptibility loci implicated in epigenetic regulation. Sci Adv. 2016;2:e1501678–e1501678.
45. Chang CC, Chow CC, Tellier LCAM, Vattikuti S, Purcell SM, Lee JJ. Second-generation PLINK: rising to the challenge of larger and richer datasets. Gigascience. 2015;4.
46. Andlauer TFM, Nöthen MM Polygenic scores for psychiatric disease: from research tool to clinical application. Medizinische Genetik;32:39–45.
47. Ge T, Chen C-Y, Ni Y, Feng Y-CA, Smoller JW. Polygenic prediction via Bayesian regression and continuous shrinkage priors. Nat Commun. 2019;10:1776.
48. Tang E, Bassett DS. Colloquium: Control of dynamics in brain networks. Rev Mod Phys. 2018;90:31003.
49. Meinert S, Repple J, Nenadic I, Krug A, Jansen A, Grotegerd D, et al. Reduced fractional anisotropy in depressed patients due to childhood maltreatment rather than diagnosis. Neuropsychopharmacology 2019;44:2065–72.
50. Benjamini Y, Yekutieli D The control of the false discovery rate in multiple testing under dependency. Ann Stat. 2001. https://doi.org/10.1214/aos/1013699998.
51. Tang E, Giusti C, Baum GL, Gu S, Pollock E, Kahn AE, et al. Developmental increases in white matter network controllability support a growing diversity of brain dynamics. Nat Commun. 2017;8:1252.
52. Cui Z, Stiso J, Baum GL, Kim JZ, Roalf DR, Betzel RF, et al. Optimization of energy state transition trajectory supports the development of executive function during youth. Elife 2020;9:1–60.
53. He X, Caciagli L, Parkes L, Stiso J, Karrer TM, Kim JZ, et al. Uncovering the biological basis of control energy: structural and metabolic correlates of energy inefficiency in temporal lobe epilepsy. Sci Adv. 2022;8:2293.
54. Stiso J, Khambhati AN, Menara T, Kahn AE, Stein JM, Das SR, et al. White matter network architecture guides direct electrical stimulation through optimal state transitions. Cell Rep. 2019;28:2554–66.e7.

55. Yang Y, Connolly AT, Shanechi MM. A control-theoretic system identification framework and a real-time closed-loop clinical simulation testbed for electrical brain stimulation. J Neural Eng. 2018;15:066007.
56. Gu S, Deng S Controllability Analysis on Functional Brain Networks. 2019:1–26.
57. Honey CJ, Sporns O, Cammoun L, Gigandet X, Thiran JP, Meuli R, et al. Predicting human resting-state functional connectivity from structural connectivity. Proc Natl Acad Sci USA. 2009;106:2035–40.
58. Jbabdi S, Johansen-Berg H. Tractography: where do we go from here? Brain Connect. 2011;1:169–83.
59. Jamalabadi H, Zuberer A, Kumar VJ, Li M, Alizadeh S, Moradi AA, et al. The missing role of gray matter in studying brain controllability. https://doi.org/10.1101/2020.04.07.030015.
60. Taghia J, Cai W, Ryali S, Kochalka J, Nicholas J, Chen T, et al. Uncovering hidden brain state dynamics that regulate performance and decision-making during cognition. Nat Commun. 2018;9:1–19.
61. Yarkoni T. Big correlations in little studies: Inflated fMRI correlations reflect low statistical power-commentary on Vul et al. (2009). Perspect Psychol Sci. 2009;4:294–8.

AUTHOR CONTRIBUTIONS

TH, UD, HJ, and JR conceived the idea and wrote the initial draft. NRW, JE, MG, MJM, LF, RL, KS, NO, DG, SM, WH, TK, IN, AJ, and UD recruited patients and acquired the data. SW, MR, MMN, AJF, BMM, TFMA processed the genetic data and provided PRS. MW, MPvdH, JR conceptualized, implemented, and conducted the DTI analysis pipeline. NRW, JE, MG, MJM, LF, RL, KS, JB, VH, DE, and MB conceptualized, implemented, and conducted the statistical and Machine Learning analysis pipelines and maintained and ran the computational infrastructure. TH, HJ, UD, and JR revised the manuscript and wrote the final version.

COMPETING INTERESTS

The authors declare no competing interests.

ETHICS APPROVAL AND CONSENT TO PARTICIPATE

The FOR2107 cohort project (WP1) was approved by the Ethics Committees of the Medical Faculties, University of Marburg (AZ: 07/14) and University of Münster (AZ: 2014-422-b-S).

ADDITIONAL INFORMATION

Supplementary information The online version contains supplementary material available at https://doi.org/10.1038/s41380-022-01936-6.

Correspondence and requests for materials should be addressed to Tim Hahn.

Reprints and permission information is available at http://www.nature.com/reprints

Publisher's note Springer Nature remains neutral with regard to jurisdictional claims in published maps and institutional affiliations.